Experimental Mechanics (2007) 47:511–521
DOI 10.1007/s11340-007-9047-7

On the Investigation of Some Parameter Identification and Experimental Modal Filtering Issues for Nonlinear Reduced Order Models

S.M. Spottswood · R.J. Allemang

Received: 19 June 2006 / Accepted: 14 March 2007 / Published online: 19 April 2007

Abstract This paper discusses modal filtering of experimental data and the corresponding identification of linear and nonlinear parameters in reduced order space. Specifically, several experimental configurations will be discussed in order to provide insight into such identification issues as spatial discretization, observability, and the linear independence of the assumed filter or basis. The two experiments considered herein represent different measurement configurations of the same clamped–clamped beam. First, asymmetric inertial loading via asymmetric sensor location was considered, while the second scenario presents a symmetric sensor configuration. Several important conclusions can be drawn from the two experimental scenarios. First, by asymmetrically loading the beam, a corresponding asymmetric beam mode was excited yet not observable. In the second scenario, the symmetric distribution of sensors minimized the impact of the respective asymmetric mode. The resulting spatial information allowed for the proper filtering of the remnants of the asymmetric mode. Nonlinear parameters in modal space as well as the underlying linear parameters were successfully identified simultaneously in both experimental scenarios, although the usefulness of the asymmetrically loaded beam was limited. Finally, successful comparisons were made between the identified reduced order model and experimental response at the beam quarter point using the symmetric case and the beam midpoint using both experimental scenarios.

Keywords Reduced order models · Identification · Duffing equations · Sonic fatigue

S.M. Spottswood (✉, SEM member)
Air Force Research Lab, AFRL/VASM,
2790 D Street,
Wright-Patterson AFB, OH 45433-7402, USA
e-mail: stephen.spottswood@wpafb.af.mil

R.J. Allemang (SEM member)
Department of Mechanical, Industrial, Nuclear Engineering,
Structural Dynamics Research Lab, University of Cincinnati,
P.O. Box 210072, Cincinnati, OH 45221-0072, USA

Introduction

Realistically speaking, there are no tractable computational tools available for the prediction of the nonlinear dynamic response of complex structures. Baring research algorithms and the analysis of trivial structures, commercially available finite element modeling (FEM) tools are not well suited to nonlinear dynamic response prediction when long time records are required. The U.S. Air Force is interested in the development of useful prediction tools for this type of problem. Details concerning the Air Force's interests and in the proposed method are discussed in [1]. Research codes principally focused on implicit or explicit means of approaching the nonlinear dynamics problem are limited in their ability to tackle realistic aircraft structures. Specifically consider the problem of an FE model in physical space incorporating solely geometric nonlinearities. For an implicit FE algorithm, the formulation of the nonlinear displacement based stiffness matrices must be accomplished at each time increment, to include convergence. While explicit algorithms do not generate a stiffness matrix per se, at each time increment (an increment only a fraction the size of the implicit one) the internal force vector must be updated. To summarize, currently available FE tools are not well suited to generate the long time records required for the type of random loading problem plaguing aerospace vehicles. While engineers await dra-

matically more powerful and efficient computing power, or more realistically, dramatically new computational tools, researchers have recently focused on approximate measures, namely nonlinear reduced order modeling. Reduced order modeling can be defined as a projection from physical degrees-of-freedom (DOF) space to some smaller subset of DOFs, all while retaining the salient physical features of the full model. While the principle of reduced order modeling is not new, the extension to include nonlinear analysis is a relatively new development. Nonlinear reduced order modeling has been used to treat nonlinear aeroelastic problems, nonlinear structural dynamic problems, and has been demonstrated useful for multi-disciplinary problems. Lucia et al. [2] discuss several reduced order modeling techniques, principally motivated by nonlinear aeroelasticity problems. These reduced order algorithms discussed, useful for prediction and design purposes, are intended to circumvent the computational burden accompanying complex full-order models, without loss of response fidelity. The purpose of this paper is to present further details and observations regarding a recently introduced method [1] primarily through experimental examples. There are limited experiments published in the literature, focused on exercising useful reduced order methods. There are even fewer references focused on experimental based nonlinear reduced order identification methods. The following references discuss some notable though certainly not exhaustive examples of each.

Kappagantu and Feeny [3–5] studied the characteristics of a frictionally excited cantilevered beam, to include the estimation of proper orthogonal modes (POM) directly from experimental displacement response [4, 5]. Proper orthogonal mode functions were obtained from the discrete POMs and used to assemble low-order ordinary differential equations. Two different response cases were used to derive the POMs, both of which exhibited chaotic behavior. The modes were obtained in the following manner. The displacement time histories were assembled into matrix form, where each column of the matrix represents a measurement location. Next, the correlation matrix was computed, the singular values and vectors of which yield the POMs. Finally, continuous modes were obtained via a Gramm–Schmidt orthonormalization technique. Numerical simulations using those models compared quite well with an expanded beam model serving as the truth model. Feeny [6] discusses the use of proper orthogonal decomposition (POD) and proper orthogonal co-ordinates (POCs) as indicators of modal activity. A cantilever beam experiment was used to examine this use of POD. Feeny also provides a succinct and useful definition of POD, "...a statistical method of finding optimal distributions of energy from a set of measurement histories." The methods outlined in [6] will be explored for the present, multi-mode nonlinear study of a clamped–clamped beam.

Azeez and Vakakis [7] utilized Karhunen–Loeve (K–L) decomposition to describe the dominant dynamic characteristics of a coupled beam problem incorporating nonlinear damping. As in the work just described, a low-order numerical model of the system described using Bernoulli–Euler beam theory was used as the truth model. K–L modes were obtained from numerical data generated from a beam model. Low-order models were generated using K–L modes and compared with low-order models generated using physical or linear normal modes. Interestingly, the model created from K–L modes required fewer modes to create a high-fidelity model of the beam structure under consideration. Of course, for this study, the system responded primarily in the first mode, greater than 99.996% of the corresponding system energy or signal power as will be discussed subsequently.

There have been several studies in the literature which investigated experimental nonlinear reduced order identification techniques useful for the type of elastic response detailed in the present study. Yasuda and Kamiya [8] present two low-order time-domain nonlinear identification techniques. Yasuda begins with an elasticity approach and arrives at the governing modal equations nonlinear in stiffness via the Galerkin Method. As in [6], the basis set is arrived at via experimental response, although in this case, weighted displacement, velocity and acceleration response histories are used. Next, the modal and forcing terms are identified. Finally, the nonlinear terms are identified via a least-squares implementation of the governing equations. The second approach simultaneously identifies all of the parameters via the minimization of an energy formulation. The authors recommend the second approach, using the first as initial conditions. A simply-supported steel beam experiment was used to compare with the proposed identifications methods. A magnetic oscillator was used to provide a fast sine-sweep input to the beam. Non-contacting optical sensors were used to measure the beam response. Good agreement was obtained between the experiment and identified model, particularly using the latter approach.

Platten et al. [9, 10] and Naylor et al. [11] applied their Nonlinear Resonant Decay Method (NL-RDM) to identify modal models for both analytical and experimental systems. The NL-RDM method is a multi-step time-domain process. First, a general sense of the linear and nonlinear characteristics of the system in question is obtained through a series of tests conducted at various input levels. The modal properties of the nominal linear system are then obtained via traditional modal testing methods. Next, the system is excited via a burst sine excitation on a mode-by-mode

basis. The excitation is applied at a level appropriate enough to exercise the nonlinearities of the respective mode. The nonlinear parameters are then identified, again on a mode-by-mode basis. The end result is a nonlinear modal model useful for prediction purposes.

Theory

The proposed method is based upon the Nonlinear Identification through Feedback of the Outputs (NIFO) Method of Adams and Allemang [12]. The NIFO method is significant in several ways. It seeks to simultaneously identify multiple nonlinear relationships between measurement locations. Further, as the method is formulated in the frequency domain, the linear components of the problem are condensed into nominal or underlying linear frequency response functions (FRF). The linear and nonlinear terms are identified on a frequency-by-frequency basis allowing for variation in the estimates as a function of frequency. As was demonstrated, this is a very useful feature, in that nonlinear parameters can be estimated in frequency regions of low variability [13]. In the proposed Modal NIFO method, an equivalent identification is accomplished, albeit in reduced order space. The usefulness of the method will be obvious, particularly with regards to mathematical models intended for prediction purposes.

The Modal NIFO method was previously described in [1] and a brief description will now follow. The key to the method is the idea that a nonlinear distributed parameter system can be appropriately modeled in a reduced order sense. So, with that assumption, consider the following nonlinear modal equation of motion for the *r*th mode of the proposed system:

$$\begin{aligned}\ddot{p}(t)_r + 2\xi_r\omega_r\dot{p}(t)_r + \omega_r^2 p(t)_r \\ + \theta_r\left(p(t)_1, p(t)_2, \ldots, p(t)_n\right) \\ = \phi_r^T f(t),\end{aligned} \tag{1}$$

where in this case θ_r represents the nonlinear portion of the expression. In the present study, the nonlinear response is of the geometric type and is most appropriately modeled by a cubic hardening stiffness. It is important to point out that the nonlinear response is intrinsic to the structure. If an implicit dynamic FE model was created to model a structure with this type of nonlinearity, then the respective physical stiffness matrix would be fully populated indicating the coupling between physical DOFs. This underscores the desire to seek an equivalent reduced order model. While the nonlinearities remain coupled, the DOFs are greatly reduced with obvious computational benefits. However it is important to point out that the localization ability of NIFO is lost in the transformation to reduced order space; that is the direct relationships between those measurement degrees-of-freedom. In the present application however, the nonlinearity is dependent on the global deformation of the structure. Local response is transformed from modal to physical space via the coupling of the retained modes used in the transformation, analogous to linear superposition. Continuing, the following cubic nonlinear geometric relationship was assumed for the present study:

$$\begin{aligned}\theta_r = \sum_{i=1}^{n} A_r(i,i,i)p(t)_i^3 \\ + \sum_{i=1}^{n-1}\sum_{j=i+1}^{n}\left\{A_r(i,i,j)p(t)_i^2 p(t)_j + A_r(i,j,j)p(t)_i\ p(t)_j^2\right\},\end{aligned} \tag{2}$$

where the A_r terms denote the nonlinear coefficients sought in the identification procedure. It is important note that only cubic nonlinear terms were retained in the present scenario. Considering nonlinear strain-displacement relations with in-plane effects in the equation of motion formulation, results in stiffness terms that are both quadratic and cubic functions of displacement. A solely cubic nonlinear modal model results when the in-plane displacements can be expressed as a function of the transverse or out-of-plane ones. Further, no more than two modes were considered in the present experimental identification cases, thus the more restricted cubic nonlinear form of equation (2) [14]. Next consider the nonlinear terms for the rth mode of a two-mode cubic model:

$$\begin{aligned}\theta_r = A_r(1,1,1)p(t)_1^3 + A_r(1,1,2)p(t)_1^2 p(t)_2 \\ + A_r(1,2,2)p(t)_1 p(t)_2^2 + A_r(2,2,2)p(t)_2^3\end{aligned} \tag{3}$$

It is also important to note that initially assuming the nonlinear form described in equation (3) is known as an implicit formulation of the sonic fatigue type nonlinear parameter identification. Recognizing the relationship between in-plane and transverse displacements allows for the initial assumption and resulting identification of the unknown nonlinear coefficients in equation (3). This is an appropriate model for the present geometric type nonlinear response, but does underscore the difficulty in any identification scenario; the act of arriving at that appropriate

nonlinear relationship. The final step in the Modal NIFO method is to transform the nonlinear modal expressions into the frequency domain and pre-multiply by the unknown *modal* FRF, $H_i(\omega)$. This results in an expression where the unknown FRF and nonlinear parameters are solved for in a normal least-squares sense. Consider such an equation for a two-mode, cubic model with four unknown A_1 terms and the unknown modal FRF, or $H_1(\omega)$:

$$\{P_1(\omega)\} = \begin{bmatrix} H_1(\omega)\ H_1(\omega)A_1(1,1,1)\ H_1(\omega)A_1(2,2,2)\ldots \\ \ldots H_1(\omega)A_1(1,1,2)\ H_1(\omega)A_1(1,2,2) \end{bmatrix} \left(- \begin{pmatrix} \left\{\widetilde{F}[f(t)]\right\} \\ \widetilde{F}\left[p(t)_1^3\right] \\ \widetilde{F}\left[p(t)_2^3\right] \\ \widetilde{F}\left[p(t)_1^2\ p(t)_2\right] \\ \widetilde{F}\left[p(t)_1\ p(t)_2^2\right] \end{pmatrix} \right), \tag{4}$$

where $\widetilde{F}[\cdot]$ denotes the Fourier Transform. Note that this expression is presented for the first mode, or $r=1$. One key step to the Modal NIFO method is the transformation of measured experimental data from physical to modal space. Since the experimental data is represented in physical space, the Moore–Penrose or pseudo inverse of the basis set, in this case populated with mass-normalized linear normal modes (LNMs), is used for the transformation. In a sense the basis set is acting as a modal filter resulting in nonlinear coupled reduced order discrete expressions analogous to equation (1). This is the principal difference between the NIFO and its related Modal method; the use of a modal filter to transform the equations of motion from physical to modal space. In order to accurately make this transformation, to arrive at a vector set that is linearly independent, and in order to accurately capture the relationships between retained modes, sufficient *experimental* spatial information must be included in the transformation. The two examples included in this study will underscore the importance of proper sensor location as well as spatial sampling.

Finally, there are several assumptions intrinsic to the Modal NIFO procedures that bear discussion. First, it is assumed that the nonlinear response of the structure can be appropriately represented in reduced order space via a limited number of mass normalized modes. These modal coordinates are of course coupled through the assumed nonlinear model, or θ_r of equations (2, 3). The linear $H_r(\omega)$ and nonlinear $A_r(\cdot)$ terms in equation (4) are identified in a normal least squares sense at each frequency. The modal transformation is accomplished using an FE derived, mass normalized basis set. Finally, the force, $F(\omega)$ must be measured, as equation (4) requires an input–output measurement relationship.

Experimental Procedure

There were two experimental configurations considered in this study. Again, the intent of the study was to demonstrate the usefulness of the Modal NIFO method in developing reduced order models, as well as to explain some of the issues users must consider when implementing the method. The experimental setup is one similar to a previous study, the purpose of which was to provide the aerospace community with a well characterized experiment useful for exercising nonlinear dynamic prediction algorithms [15]. As previously mentioned, the idea of developing these useful tools has been going on for some time. Over the years, numerical and experimental sonic fatigue type comparisons have been made, although at the time there was no high-fidelity case-study presented in the literature that was useful for this type of aerospace structural response. The experiments in the present study represent two configurations of the same beam structure. In both instances, the desired outcome was a reduced order model of the beam to be used for predicting the response of the beam midpoint and quarter-point for a loading scenario different than that used for identification. The experimental setup and beam characteristics are shown in Fig. 1.

The beam was a high-carbon steel precision feeler gage, inserted into a steel clamping fixture. The first configuration, Case 1 has the sensors positioned on only one-half of the beam, as noted in Fig. 1. This configuration was intended to demonstrate the issues of asymmetric loading, spatial discretization, and modal observability. In the second experimental configuration, Case 2, the sensors

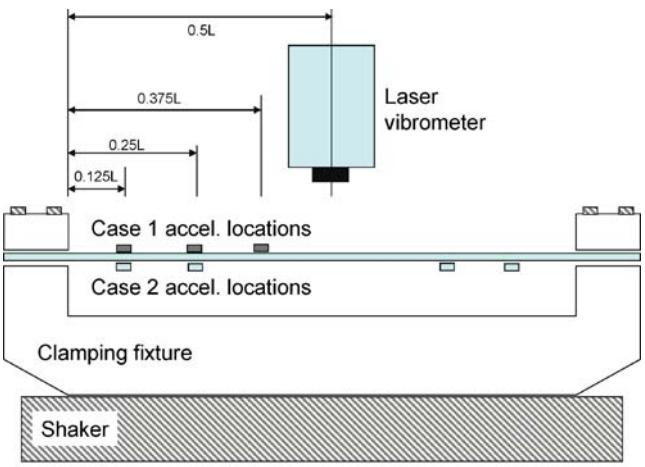

Length: 2.29e-1 m (9.0 in)
Thickness: 8.13e-4 m (0.032 in)
Width: 1.27e-2 m (0.5 in)
Mass Density: 7872 kg/m^3 (7.36e-4 lb-s^2/in^4)
Elastic Modulus: 205 GPa (29.7e+6 lb/in^2)

Fig. 1 Experimental setup and beam characteristics

were reattached symmetrically along the beam span. In both cases, a laser vibrometer was used to record the beam midpoint velocity, numerically integrated to arrive at the desired midpoint displacement. Thus, in addition to the beam midpoint response, Case 1 included three accelerometers, while Case 2 included a total of four accelerometers. In both cases, the number of independent measurement locations exceeded the number of modes retained in the filter. The accelerometer data was twice integrated in the frequency domain to arrive at the desired displacement response. As this type of pseudo-integration can result in low-frequency numerical problems, data below the lower-band driving frequency was omitted. The respective measurement locations for the two cases represent points along the beam intended to allow for linear independence of the basis set used for the transformation to modal space. The location of the sensors for Cases 1 and 2 are displayed in Fig. 2, along with the first three LNMs used for the modal filtering.

Singular value decomposition (SVD) is another useful tool frequently utilized in reduced order modeling. SVD can provide for a relative measure of the energy content of the respective modes. Figure 3 presents the normalized singular values for Cases 1 and 2 at two different loading conditions, 4 g's used in the forthcoming identification, and 9 g's used to compare with the identified reduced order models.

In each case, the first two POMs dominate the response in terms of their signal power, or the respective significance of the corresponding proper orthogonal values (POVs). The POMs are the optimal distributions of signal power, and the respective POVs represent the corresponding amount of signal power [6]. Figure 4 displays the first two experimentally derived POMs for Cases 1 and 2, versus the LNMs utilized in the modal filter.

The cumulative power, described subsequently, of the first two POMs derived from the measured response of the 4 g loading, was calculated to be 99.94% for Case 1 and 99.91% for Case 2. A procedure similar to [6, 8] was used to arrive at the POMs and the respective signal power calculations. First, the experimental measurements were integrated in the frequency domain in order to arrive at the

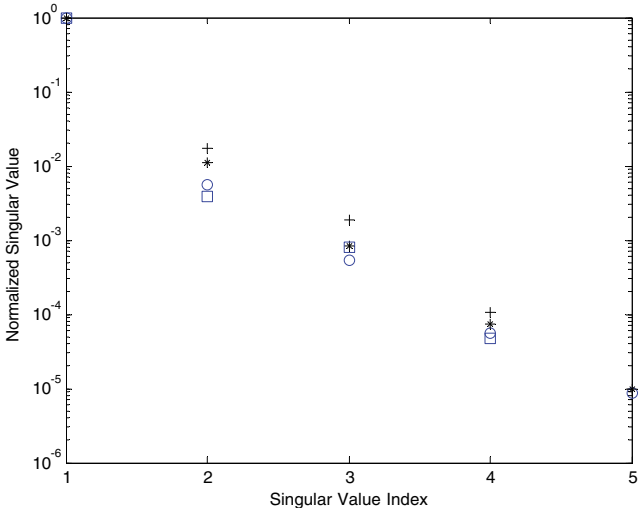

Fig. 3 Singular values for Case 1 and 2 experimental data (*square*: Case 1 4 g load; *cross*: Case 1 9 g load; *circle*: Case 2 4 g load; *asterisks*: Case 2 9 g load)

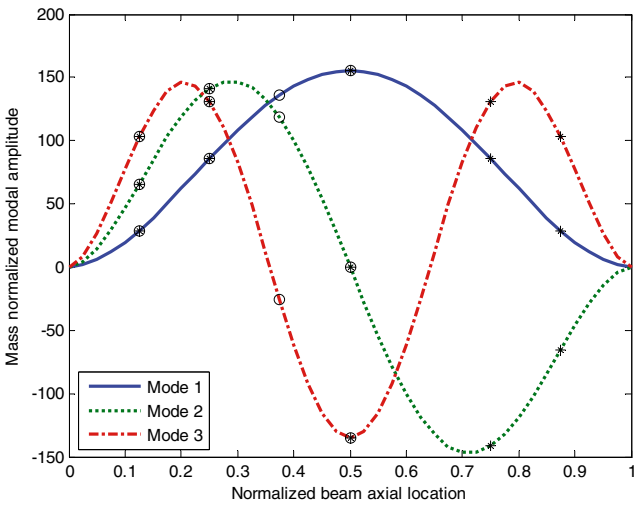

Fig. 2 First three beam bending normal modes and sensor locations used in the modal transformation (*circle*: Case 1 sensor location; *asterisks*: Case 2 sensor location)

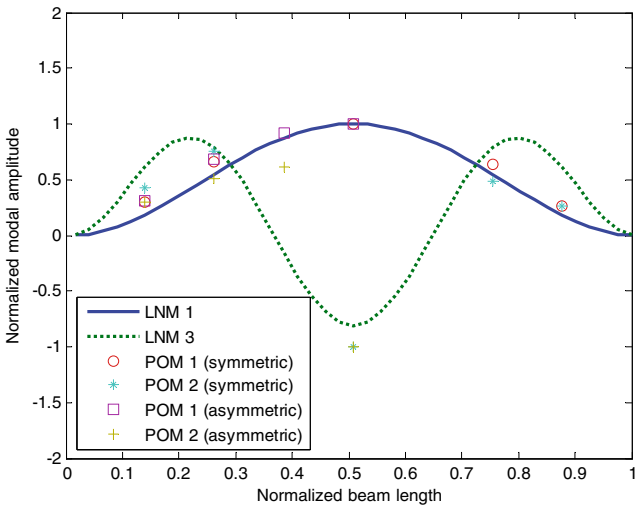

Fig. 4 Linear normal modes (*LNM*) versus experimentally derived proper orthogonal modes (*POMs*) (*solid line*: linear normal first mode; *dashed line*: linear normal second mode; *circle*: POM 1 symmetric data; *asterisks*: POM 2 symmetric data; *square*: POM 1 asymmetric data; *cross*: POM 2 asymmetric data)

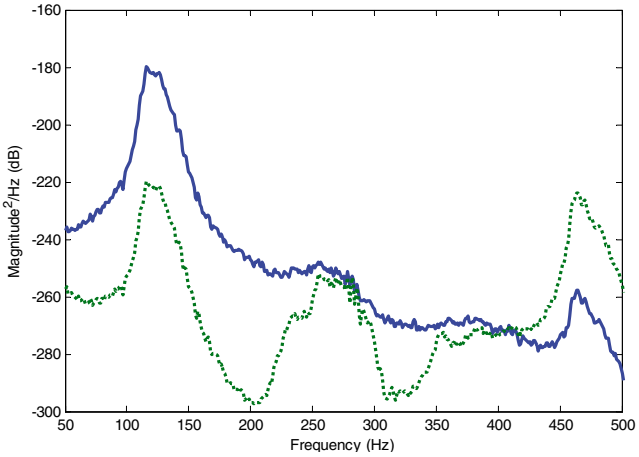

Fig. 5 Modal filter results for Case 1, asymmetric loading and filter (*solid line*: Mode 1; *dotted line*: Mode 3)

desired displacements. Next, for each case, the displacement time histories of length N were assembled into the following **N**×**M** ensemble matrix:

$$[X] = [x_1(t)\ x_2(t)\ \ldots\ x_M(t)] \tag{5}$$

As in [6], the correlation matrix was calculated and the singular values and vectors of that matrix were obtained:

$$[R] = 1/N[X]^T[X] \tag{6}$$

The correlation matrix [**R**] is both symmetric and positive semi-definite indicating the eigenvalues are real and nonnegative. The resulting orthonormal singular vectors of this matrix are equivalent to the POMs. The signal power of the respective *i*th mode is represented in the following relation:

$$\lambda_i = v_i \Big/ \sum_{j=1}^{n} v_j, \tag{7}$$

where v represents the normalized singular value and n the total number of modes. The power of multiple modes can be considered via the cumulative effect of equation (7). This idea of using the cumulative power of the POVs has been used as a measure of the activity of the respective POMs [6]. At the present time, LNMs derived from FEA were used in the Modal NIFO identification procedure, however in on-going work the authors will consider the use of a weighted basis via experimentally derived POMs. This would provide snapshots of the state of the system under actual measurement conditions. Note in Fig. 3 that the relative contribution of the second and even the third POM increase with increasing loading. What is most striking is the relative increase in the third POM for Case 1 at the 9 g load scenario. This is the case that includes significant asymmetric influence from the sensor location. One important point to be made regarding the experiment is the influence of the accelerometers on such a small structure. While non-contacting measurement devices would be most appropriate, it was interesting to observe how the use of these micro-accelerometers to identify nonlinear parameters influenced the prediction scenarios. As will be discussed shortly, the underlying linear system and therefore the influence of the sensors, was also successfully identified.

A broadband random excitation method was selected to exercise the nonlinear response of the beam. The shaker was oriented in a horizontal fashion in order to minimize the effect of gravity on the beam response. While random excitation is not typically utilized for experimental nonlinear characterization, the premise of the proposed modal filtering method assumes the ability to separate the nonlinear response into their respective modal contributions. Recall that the nonlinear modal expressions presented and discussed earlier, are coupled in terms of the respective nonlinear parameters. Further, the intent of the Modal NIFO method is to identify these nonlinear parameters as functions of frequency. Rather than exciting the beam structure at each of the relevant modes it was deemed more appropriate in an MDOF identification sense to provide as much nonlinear information across the frequency band as possible. In traditional modal analysis, random excitation in conjunction with a Hanning Window is a popular excitation approach. This is true even when better test scenarios are available, namely those that more appropriately satisfy both the assumed linear transfer function (rational fraction polynomial) as well as the oft used Fast Fourier Transform (FFT). Thus, it was with purpose that a broadband random excitation was selected, the purpose being to apply energy equally over the desired bandwidth in order to exercise as much of the geometric nonlinear characteristics as possible. Finally, a tensile preload was applied to the beam to mitigate any curvature effects. This was accomplished by

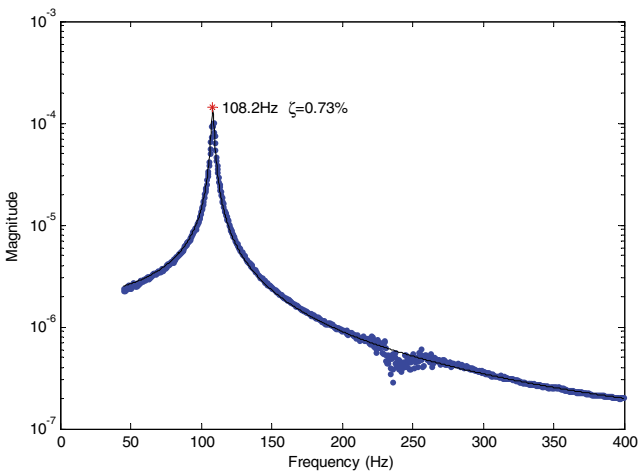

Fig. 6 Mode 1 nominal nonlinear system estimates

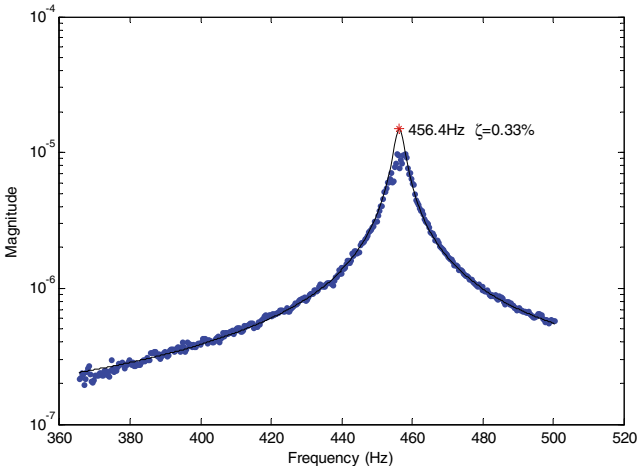

Fig. 7 Mode 3 nominal nonlinear system estimates

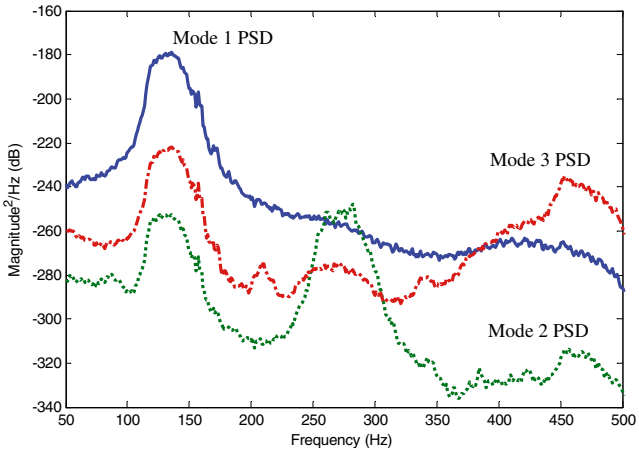

Fig. 8 Modal filter results for Case 2, symmetric loading and filter (*solid line*: Mode 1; *dotted line*: Mode 2; *dash-dot line*: Mode 3)

heating the beam slightly and allowing the beam to cool once fastened into the clamping fixture. The nominal, unstressed fundamental frequency occurs at 78 Hz. The first mode was increased to approximately 110 Hz as a result of the tensile preload.

Results and Discussion

The Modal NIFO procedure occurs as follows; first, the experimental data is filtered and scaled by the desired physical response point along the beam. Next, the data is transformed into the frequency domain and assembled into a form appropriate for identification as displayed in equation (4). Finally, the nonlinear parameters and underlying linear system are identified simultaneously on a frequency-by-frequency basis. The results of the two experimental scenarios are now presented. Consider first the results of Case 1, where only half the beam response was captured. Figure 5 displays the raw modal displacement results from the filtering of Case 1, where a uniform 4 g RMS load between 40 and 500 Hz was applied.

Recall that the only the first two *symmetric* modes, modes 1 and 3 were used in the filter for Case 1. The choice of this particular basis was to ensure the independence of the basis. Due to the sensor locations and thus the physical DOFs used in the modal filter, the first asymmetric mode, mode 2, was linearly related to both symmetric ones. Note that the response power spectral densities (PSDs) representing the two nonlinear modal expressions, indicate significant response between 200 and 300 Hz. This response is not an artifact of the nonlinear system, but is due to some phenomenological influence not included in the transformation. What is occurring is the excitation of the first *asymmetric* mode, exacerbated by the asymmetric location of the sensors. Now consider Figs. 6 and 7, the linear results of the Modal NIFO identification procedure for the first two symmetric modes of Case 1.

Recall that in the assumed nonlinear model, there were two assumed cubic nonlinear modal expressions, representing a total of eight nonlinear constant parameters. Spectral averages of the real components of the nonlinear coefficients for the symmetric modes are presented in Table 1. Just to reiterate, Figs. 6 and 7 were identified at the same time as the nonlinear parameters displayed in Table 1. The identification results of [1] provided solely the nonlinear parameters. In the present study, the linear estimates were used in the response prediction, to be discussed shortly.

The results of the modal filtering for Case 2 are presented in Fig. 8, now using all three modes in the transformation to modal space. The loading conditions were nominally the same as for Case 1.

The modal response noted earlier between 200 and 350 Hz is no longer apparent in the symmetric modal response of Fig. 8. The effect of any asymmetric beam loading has been appropriately captured by the now included asymmetric mode. It is interesting that this mode is actually being excited, as the sensors are symmetrically positioned along the beam. What is important to note is that the response of the asymmetry has been removed from the data intended for identification. The data represented in Figs. 5 and 8, are the modal PSDs. The transformation back

Table 1 Nonlinear coefficients for asymmetric two-mode model, $m^{-2}s^{-2}$ ($in^{-2}s^{-2}$)

Mode 1	Mode 3
$A_1(1,1,1)$=2.15e11(1.39e8)	$A_2(1,1,1)$=2.12e11(1.37e8)
$A_1(1,1,2)$=6.05e11(3.90e8)	$A_2(1,1,2)$=1.84e12(1.19e9)
$A_1(1,2,2)$=2.51e12(1.62e9)	$A_2(1,2,2)$=5.30e12(3.42e9)
$A_1(2,2,2)$=5.46e12(3.52e9)	$A_2(2,2,2)$=9.64e12(6.22e9)

to physical space would appropriately scale this data to represent the respective spatial information. For instance, in both Cases 1 and 2, the response of the beam midpoint is principally due to the symmetric modes. The influence of the asymmetric mode is negligible as will be discussed shortly. If however, the effect of the asymmetric mode is not removed as it was for Case 2 and displayed in Fig. 8, then the appropriate scaling can not take place resulting in unintended influence or bias.

The linear identification results for the symmetric modes are presented in Figs. 9 and 10.

It is important to point out that in both identification scenarios, Cases 1 and 2, equation (4) was scaled by the beam midpoint using the standard modal expansion formulation. Nonlinear parameters associated with the asymmetric mode were not included in the nonlinear model. At the beam midpoint, the response of the asymmetric mode is negligible and thus not represented in the identification results. The nonlinear parameter results of Case 2 identification scenarios are presented in Table 2.

Given the linear and nonlinear identification results of Cases 1 and 2, modal models were assembled and compared with the beam experimental response at nearly 9 g's RMS loading. Recall that the loading scenario used in both cases was nominally 4 g's. In all instances, broadband random loading between 40 and 500 Hz was used to excite the numerical models and generate 100 s of response data. Comparisons were made at both the beam midpoint as well as the beam quarter point, where any asymmetric effects would be exacerbated (see the relative modal scaling of Fig. 2). For Case 1, the assembled modal models included modal damping values and frequencies of 0.73% at 108 Hz and 0.33% at 456 Hz for the first and third modes. For Case 2, the assembled modal models included modal damping values and frequencies of 0.44% at 113 Hz and 0.60% and 447 Hz, respectively. The differences in the underlying

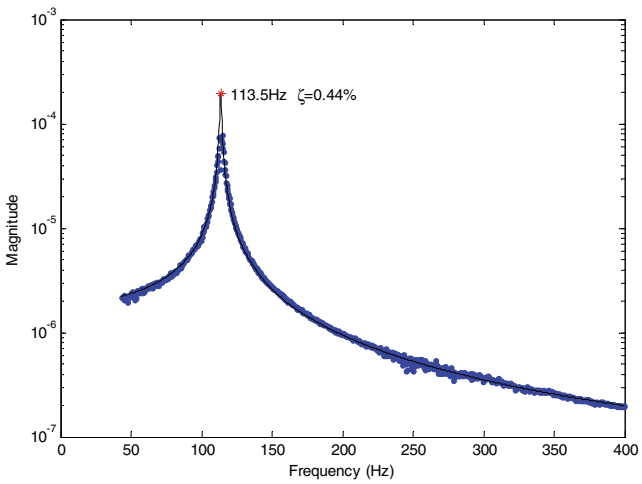

Fig. 9 Mode 1 nominal linear system estimates

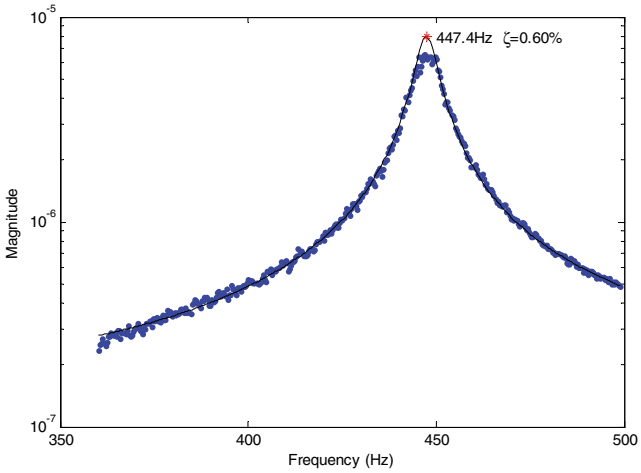

Fig. 10 Mode 3 nominal linear system estimates

linear system parameters are due to changes in the ambient conditions during testing (the beam is very sensitive to small changes in temperature), as well as the differences in numbers and location of sensors for each of the cases. The nonlinear parameters represented in Tables 1 and 2, were used to complete the assembly of the nonlinear modal models, the form of which is displayed in equation (1). It can not be overemphasized that all of the prediction results presented herein, were generated from models identified solely from experimental data. There was no tuning of the boundary conditions or linear parameters to present 'better' comparisons. Every parameter used to assemble the respective modal models was identified from experimental data. Finally, the assumed modal basis used in the transformation from physical to modal coordinate's utilized mass normalized analytic mode shapes. Although experimentally derived mode shapes were not used in the transformation, nothing precludes their use given appropriate modal scaling for the assumed model.

Consider first the prediction results displayed in Fig. 11. These results compare the assembled nonlinear modal model for Case 1 and the respective experimental configuration at 9 g's. While there are slight discrepancies between the prediction and experimental response, the prediction is quite good as evidenced by a comparison of RMS displacement values; 8.38e−4 m (0.033 in) for each case.

Table 2 Nonlinear coefficients for symmetric two-mode model $m^{-2}s^{-2}$ ($in^{-2}s^{-2}$)

Mode 1	Mode 3
$A_1(1,1,1)$=2.05e11(1.32e8)	$A_2(1,1,1)$=2.71e11(1.75e8)
$A_1(1,1,2)$=6.56e11(4.23e8)	$A_2(1,1,2)$=2.43e12(1.57e9)
$A_1(1,2,2)$=4.46e12(2.88e9)	$A_2(1,2,2)$=6.35e12(4.10e9)
$A_1(2,2,2)$=1.60e13(1.03e10)	$A_2(2,2,2)$=1.60e13(1.03e10)

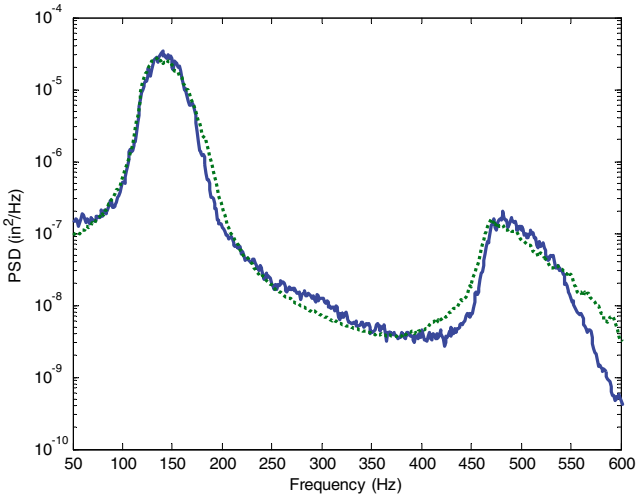

Fig. 11 Beam midpoint response to 9 g loading using experimentally derived linear and nonlinear parameters from Case 1 (*solid line*: experimental response; *dotted line*: predicted response)

Next, consider the quarter-point response prediction of Fig. 12. In this case, the effect of the asymmetry and the inability to capture that effect is obvious. Interestingly, a comparison of the displacement response RMS values is quite good; 5.84e−4 m (0.023 in) versus 5.33e−4 m (0.021 in), respectively. This underscores the fact that this beam structure primarily responds in the first mode, where for even the quarter-point, the comparison is quite good.

Consider next, the same quarter-point beam comparison where the results are now presented in their respective modal contributions, Fig. 13.

Again, note that the prediction, a two symmetric mode model, completely misses the asymmetric response between 250 and 350 Hz. This asymmetric effect can not be captured due to the limited spatial nature of the measurement DOFs for Case 1. The effect of this asymmetric

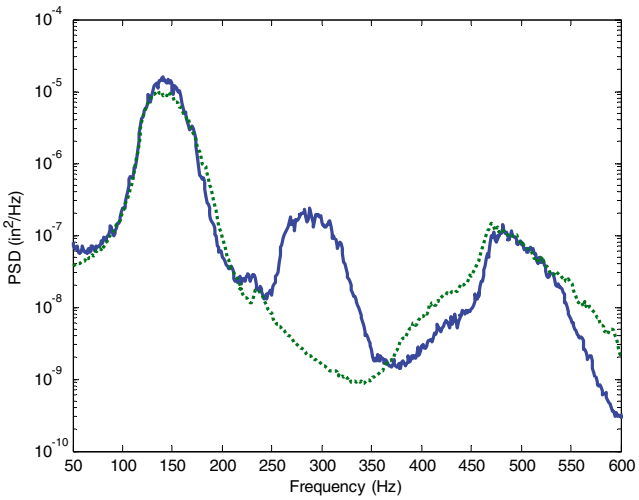

Fig. 12 Beam quarter-point response to 9 g loading using experimentally derived linear and nonlinear parameters from Case 1 (*solid line*: experimental response; *dotted line*: predicted response)

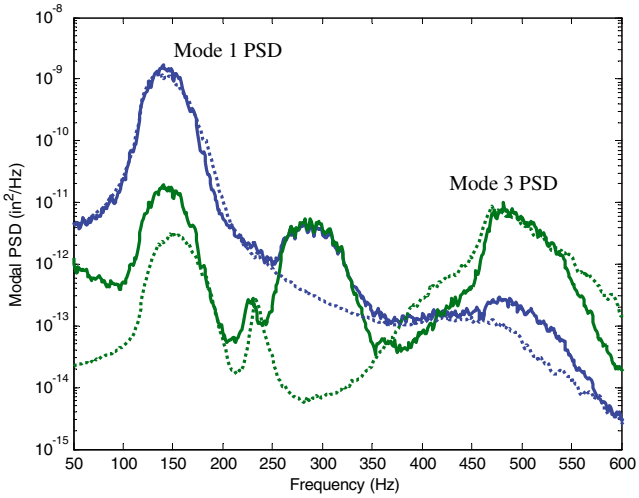

Fig. 13 Beam quarter-point modal response to 9 g loading using experimentally derived linear and nonlinear parameters from Case 1 (*solid line*: experimental modal response; *dotted line*: predicted modal response)

loading can be further explored in the following numerical example. In this case, a 40-element nonlinear dynamic FE model of the beam was assembled utilizing a direct evaluation reduced order approach [14]. The nonlinearity in the FE model is found in the large displacement and rotation response of the beam elements. Broadband random loading was prescribed, and 100 s of response calculated using a Newmark–Beta numerical integration scheme. The model mass was perturbed at the Case 1 sensor locations in order to introduce qualitatively similar asymmetrical effects. Next, the physical response of the numerical model was filtered using the aforementioned pseudo-inverse procedure using FE DOFs for half of the beam, analogous to Case 1. Figure 14 presents the Case 1 modal filtering results for this numerical experiment.

Note that this numerical filtering example representing only half the beam has incorporated the asymmetry into the

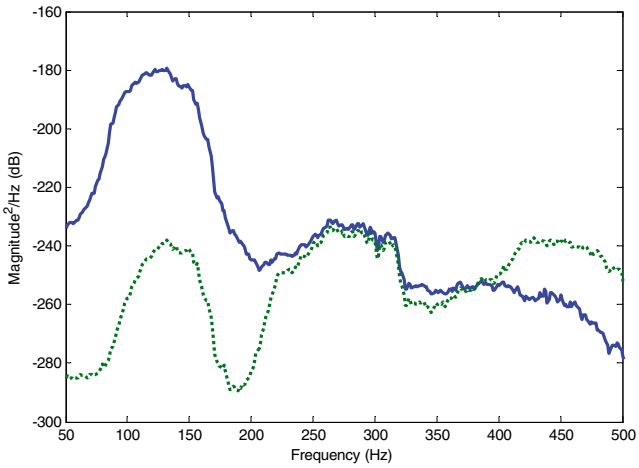

Fig. 14 Numerical modal filter results for asymmetric loading and filter (*solid line*: Mode 1; *dotted line*: Mode 3)

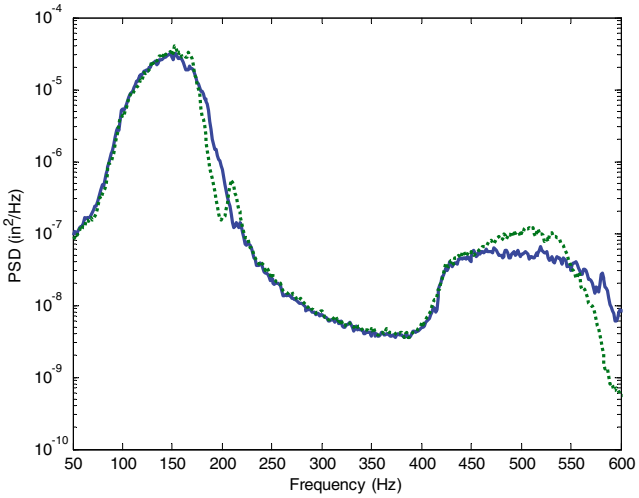

Fig. 15 Numerical beam midpoint response to 8 g loading using experimentally derived linear and nonlinear parameters from Case 1 (*solid line*: experimental response; *dotted line*: predicted response)

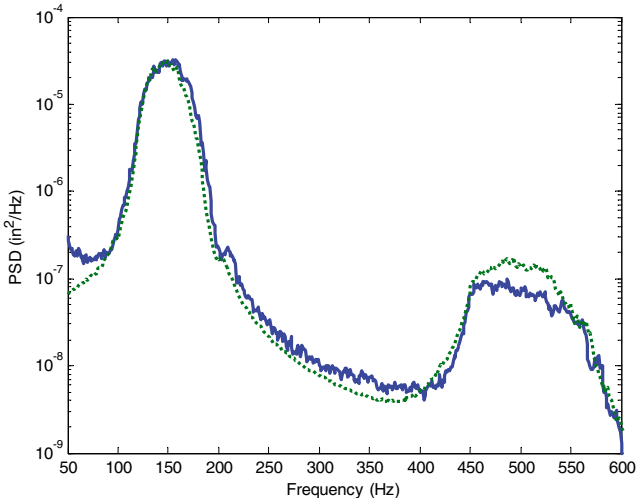

Fig. 17 Beam midpoint response to 9 g loading using experimentally derived linear and nonlinear parameters from Case 2 (*solid line*: experimental response; *dotted line*: predicted response)

symmetric mode response as in the experimental filtering of Fig. 5. To complete this numerical example, the beam midpoint and quarter point numerical data was compared with a reduced order model identified from the numerical experiment. The loading condition used for the identification was consistent with what was used for the actual experiment. The results of this comparison are presented in Figs. 15 and 16.

Note that at the beam midpoint, the affect of the asymmetry is negligible, while at the quarter point, the affect is quite striking, just as in Case 1 of the experiment. The model identified using only one-half of the spatial information clearly can not capture the asymmetric loading effect. This numerical example serves to qualitatively demonstrate the importance of spatial discretization as well as the principle of observability. For the half-beam filter, the asymmetric mode looks strikingly similar to the two symmetric ones used in the filter, and therefore its effect is absorbed into the symmetric modes. Even though the mode has been excited, it is not observable in the assumed configuration.

Next, consider the experimental results of Case 2, where the accelerometers were symmetrically located along the beam surface. Figures 17 and 18 display the midpoint and quarter-point comparison results for Case 2. Beam midpoint and quarter-point comparisons are very good, both when comparing spectra as well as RMS displacement results; 9.40e−3 m (0.37) and 8.64e−3 m (0.34 in), and 6.35e−4 m (0.025) and 5.33e−4 m (0.021 in), respectively. For both beam locations, the predicted response was marginally lower than the actual experimental response. This small difference in RMS displacement results can be attributed to

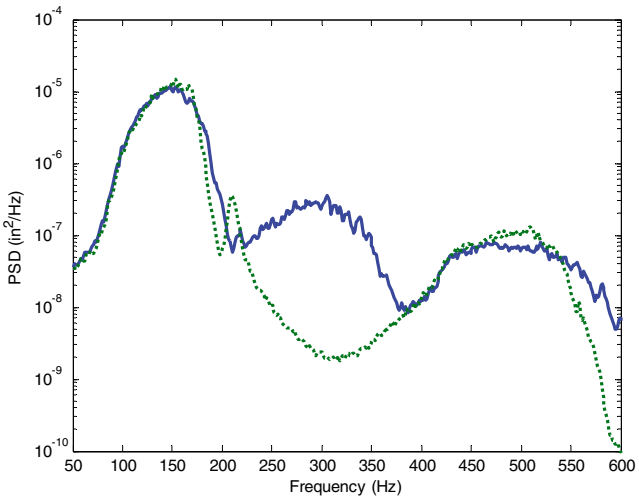

Fig. 16 Numerical beam quarter-point response to 8 g loading using experimentally derived linear and nonlinear parameters from Case 1 (*solid line*: experimental response; *dotted line*: predicted response)

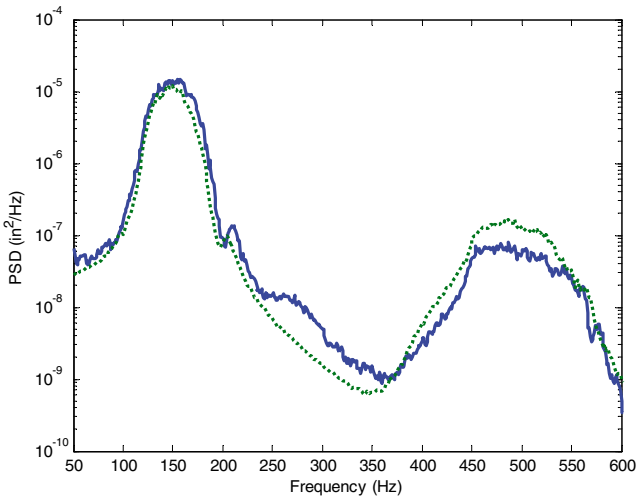

Fig. 18 Beam quarter-point response to 9 g loading using experimentally derived linear and nonlinear parameters from Case 2 (*solid line*: experimental response; *dotted line*: predicted response)

the seemingly small differences in the predicted first mode response of Figs. 17 and 18.

Conclusion

The ability to assemble accurate nonlinear reduced order models from experimental data is important in understanding the response of aircraft structures to high-intensity, random loading. This study demonstrates a useful method to obtain those reduced order models through experimental and numerical examples. The Modal NIFO method captures the underlying linear and nonlinear system simultaneously, a useful capability, particularly when dealing with sensitive experimental configurations. Several experimental configurations were studied in order to explain some complications, namely spatial discretization and observability that can arise from improper measurement location as well as their unnecessary influence on the structure of interest. It was observed that improper sensor location excited an unwanted asymmetric mode. Further, proper sensor location provides the means for removing through filtering, nominal experimental asymmetric effects. Excellent agreement was achieved between highly-nonlinear experimental results and identified nonlinear reduced order models at the beam midpoint for all experimental scenarios considered, and at the beam quarter-point for the symmetric experimental configuration. The same can not be said for the beam quarter-point comparison where asymmetric sensor placement exacerbated intrinsic effects in the beam, resulting in a poor spectral comparison. In all instances, RMS values compared quite well, indicating the relative insensitivity of that particular statistical measure. Finally, a numerical experiment using a nonlinear FE method was conducted in order to demonstrate that the asymmetric beam response can be modeled via asymmetric loading analogous to the Case 1 sensor locations. Successful qualitative comparisons were made between this numerical example and the experimental results of Case 1.

References

1. Spottswood SM, Allemang RJ (2006) Identification of nonlinear parameters for reduced order models. J Sound Vib 295:226–245.
2. Lucia DJ, Beran PS, Silva WA (2004) Reduced-order modeling: new approaches for computational physics. Prog Aerosp Sci 40:51–117.
3. Kappagantu RV, Feeny BF (1999) An optimal modal reduction of a system with frictional excitation. J Sound Vib 224:863–877.
4. Kappagantu RV, Feeny BF (2000) Part 1: dynamical characterization of a frictionally excited beam. Nonlinear Dyn 22:317–333.
5. Kappagantu RV, Feeny BF (2000) Part 2: proper orthogonal modal modeling of a frictionally excited beam. Nonlinear Dyn 23:1–11.
6. Feeny BF (2002) On proper orthogonal co-ordinates as indicators of modal activity. J Sound Vib 255:805–817.
7. Azeez MFA, Vakakis AF (2001) Proper orthogonal decomposition (POD) of a class of vibroimpact oscillations. J Sound Vib 240:859–889.
8. Yasuda K, Kamiya K (1999) Experimental identification technique of nonlinear beams in time domain. Nonlinear Dyn 18:185–202.
9. Platten MF, Wright JR, Cooper JE, Sarmast M (2002) Identification of multi-degree of freedom non-linear simulated and experimental systems. Proceedings of the international conference on Noise and Vibration Engineering (ISMA 2002), Leuven, pp 1195–1202 (September).
10. Platten MF, Wright JR, Cooper JE (2004) Identification of a continuous structure with discrete non-linear components using an extended modal model. Proceedings of the international conference on Noise and Vibration Engineering (ISMA 2004), Leuven, pp 2155–2168 (September).
11. Naylor S, Platten MF, Wright JR, Cooper JE (2004) Identification of multi-degree of freedom systems with nonproportional damping using the Resonant Decay Method. J Vib Acoust 126:298–306.
12. Adams DE, Allemang RJ (2000) A frequency domain method for estimating the parameters of a non-linear structurally dynamic model through feedback. Mech Syst Signal Process 14:637–656.
13. Spottswood SM, Allemang RJ (2006) Identification of nonlinear parameters for reduced order models. Proceedings of the ninth international conference on recent advances in structural dynamics, Southampton, July.
14. Hollkamp JJ, Gordon RW, Spottswood SM (2003) Nonlinear sonic fatigue response prediction from finite element modal models: a comparison with experiments, AIAA-2003-1709.
15. Gordon RW, Hollkamp JJ, Spottswood SM (2003) Nonlinear response of a clamped–clamped beam to random base excitation. Proceedings of the eighth international conference on recent advances in structural dynamics, Southampton, July.